Significance of trends in gait dynamics

Klaudia Kozlowska [1,‡], Miroslaw Latka[1,‡*], Bruce J. West[2,‡]

1 Department of Biomedical Engineering, Wroclaw University of Science and Technology, Wroclaw, Poland

2 Army Research Office, Information Sciences Directorate, Research Triangle Park, USA

* Corresponding author

E-mail: Miroslaw.Latka@pwr.edu.pl

‡These authors contributed equally to this work.

Abstract

Trends in times series generated by physiological control systems are ubiquitous. Determining whether trends arise from the intrinsic system dynamics or are an epiphenomenon originating outside system is the fundamental problem in fractal series analysis. In the latter case, it is necessary to filter out the trends before attempting to quantify correlations in the noise (residuals). For over two decades, detrended fluctuation analysis (DFA) has been used to calculate scaling exponents of stride time (ST), stride length (SL), and stride speed (SS) of human gait. Herein, rather than relying on the very specific form of detrending characteristic of DFA, we adopt Multivariate Adaptive Regression Splines (MARS) to explicitly determine trends in spatio-temporal gait parameters during treadmill walking. Then, we use fluctuation analysis (FA) to calculate the scaling exponent of the corresponding MARS residuals. The durations of ST and SL trends are determined to be independent of treadmill speed and have a quasi-exponential distribution. At all speeds considered, the trends of ST and SL are strongly correlated and are statistically independent from their corresponding residuals. The group-averaged values of scaling exponents of ST and ST MARS residuals are smaller than 0.5, indicating anti-persistence, which is to say that a positive (negative) fluctuation is preferentially followed by a negative (positive) fluctuation. Thus, contrary to the prevalent interpretation in the literature, the persistence of ST and SL does not necessarily follow from the properties of residuals, but rather from those of trends. The presented results resolve two paradoxes of treadmill gait, namely that ST and SL are not only weakly coupled, but weakly controlled as well. We argue that intermittent control gives rise to trends in ST and SL, and the values of such trends serve as control points about which the corresponding gait parameters anti-persistently fluctuate.

Author summary

Statistical persistence of stride time (SL) and stride length (SL) during treadmill walking is an intriguing property of human gait. For persistent fluctuations, any deviation from the mean value is likely to be followed by a deviation in the same

direction. Thus, ST and SL seem to be weakly controlled which is counter-intuitive for anyone who ever stepped on a treadmill. To trace the origin of the paradox, we used a novel approach to determine trends in spatio-temporal gait parameters. We find that the trends of ST and SL of a subject are strongly correlated and are statistically independent from their corresponding residuals. In sharp contrast to previous studies, it is shown that persistence of SL and ST fluctuations results, not from the properties of residuals, which on average are anti-persistent, but rather from those of the trends. The results presented offer a new interpretation of the control of gait parameters. Intermittent control gives rise to trends in ST and SL, and the values of such trends serve as control points about which the corresponding gait parameters fluctuate in an anti-persistent manner.

Introduction

Over two decades ago Hausdorff et al. [1, 2] discovered long-range, persistent correlations in stride duration (time) of human gait. Their choice of fractional Brownian motion (FBM) [3] for modelling such correlations has significantly influenced the way in which fluctuations of spatio-temporal gait parameters (stride time, stride length, and stride speed) were subsequently quantified and interpreted. Determining the source of ubiquitous trends observed in physical, social, or biological systems is a recurring problem in fractal time series analysis. In other words, one has to establish whether trends arise from the intrinsic dynamics of a system or are an epiphenomenon of external origin. In the latter case, a possible approach is first to recognize trends and then filter them out before attempting to quantify correlations in the noise (residuals). In their original study Hausdorff et al. applied detrended fluctuation analysis (DFA) [4] to estimate the scaling (Hurst) exponent, which characterizes properties of fractal time series. Their choice of DFA implied that a stride duration time series was made up of persistent (scaling exponent greater than 0.5) fractal fluctuations superposed on irrelevant, from the point of view of fractal analysis, trends. In other words, by using DFA it was implicitly assumed that the trends were not generated by motor control and therefore were not part of the fractal process generating the fluctuations.

The papers of Hausdorff et al. spurred significant interest in the emerging field of

fractal physiology [5, 6]. In particular, they focused research on the intrinsic variability of physiological time series and their persistence [7]. Some argued that persistent fluctuations are a manifestation of the adaptability of underlying control systems and the absence of long-range correlations, or anti-persistence, indicates disease or pathology [8–10]. Delignières and Torre demonstrated that when healthy humans walk over ground in sync with a metronome, their stride times become anti-persistent [11]. During treadmill walking, a subject's stride time (ST) and stride length (SL) must yield a stride speed (SS) that fluctuates over only a narrow range, centered on the treadmill belt's speed. It turns out that subjects' SS is anti-persistent, while the other two gait parameters, ST and SL, are persistent. On the other hand, all three parameters are anti-persistent during treadmill walking with either auditory [12] or visual [13] cueing (alignment of step lengths with markings on the belt). In light of these latter experimental findings, anti-persistence, rather than being a manifestation of pathology, seems to be indicative of tight control.

The weak control of stride time and speed during uncued walking, as manifested by the persistence of both parameters, is counter-intuitive for anyone who ever stepped on a treadmill. Another puzzling property of gait dynamics, which is worth mentioning at this point, is the weak coupling between stride time and stride length measured by cross-correlation. The coefficient of correlation between these dynamical variables for uncued treadmill walking is 0.28 and increases to approximately 0.55 under the influence of a persistent fractal metronome [14]. Herein, we employ an explicit algorithm to determine trends in spatio-temporal gait parameters and examine their statistical properties as well as those of the corresponding residuals. In the process, light is shed on the two previously mentioned paradoxes of treadmill gait: the weak coupling between ST and SL, and the origin of their persistence.

Results

ST and SL trends

The examples of stride time, length and speed time series are given in Fig 1. The solid, thick lines in this figure represent trends approximated using the piecewise linear

variant of the MARS model. The Kruskal-Wallis test showed that durations of normalized trends (durations divided by the subject's mean value of stride time or stride length) were independent of treadmill speed. For stride time, $p_{ST} = 0.33$. For stride length, $p_{SL} = 0.04$, but the post hoc analysis did not reveal any statistically significant differences. Therefore, we aggregated data from all the trials. The average values and standard deviations of trend durations were very close to each other (35.66 and 35.87 for stride time, and 32.21 and 35.00 for stride length). The fundamental property of exponential distribution whose probability density function (PDF) is equal to $exp(-\lambda x)\lambda$ is that its average value and standard deviation are both equal to $1/\lambda$. Therefore, in Fig. 2 we present PDFs of trend durations along with the exponential PDFs fitted to the experimental data. The parameters of the exponential distributions were $\lambda_{ST} = 0.028$ ($1/\lambda_{ST} = 35.52$) and $\lambda_{SL} = 0.031$ ($1/\lambda_{SL} = 32.17$) for stride time and stride length, respectively. It is apparent from the probability plots, presented as insets in Fig. 2, that the differences between the experimental and exponential distributions are the largest at short trend durations. The Anderson-Darling test showed that the experimental samples of ST and SL trend durations were not drawn from an exponential distribution ($p_{ST} = 2 \times 10^{-6}$ and $p_{SL} = 5 \times 10^{-7}$). The same test showed that the ST and SL trend duration distributions, while being quite similar to each other, were in fact statistically different ($p = 6 \times 10^{-7}$).

The MARS algorithm did not find any trends in stride speed time series.

Scaling exponents

The mean values of ST, SL, and SS scaling exponents at different treadmill speeds are presented in Table 1 along with the corresponding standard deviations. All indices that are statistically smaller than 0.5 are marked with the dagger symbol. The parameters $\alpha^{(0)}$, $\alpha^{(1)}$, and $\alpha^{(2)}$ are exponents calculated using detrended fluctuation analysis of order 0 (DFA0), 1 (DFA1), and 2 (DFA2), respectively. The parameter $\alpha^{(FA)}$ was computed using the fluctuation analysis (FA). Scaling analysis was performed for the raw experimental time series and time series detrended using the piecewise linear variant of the MARS model. In the latter case, the exponents have a L subscript. Fig. 3 displays the results of the scaling analysis for ST and SL time series.

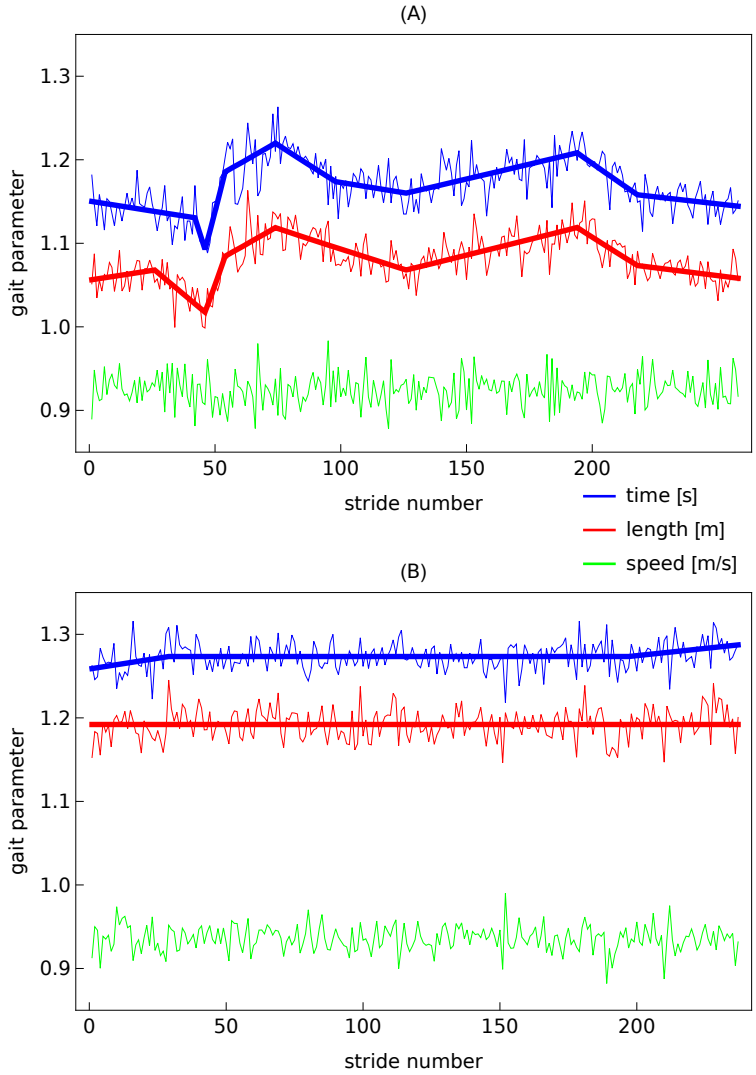

Fig 1. Stride time, length and speed of two healthy, young subjects during treadmill walking at a preferred walking speed: (A) subject 6, trial 2, (B) subject 1, trial 2. Solid lines show trends calculated using the piecewise linear variant of the MARS model. Experimental data come from the study of Dingwell et al. [15].

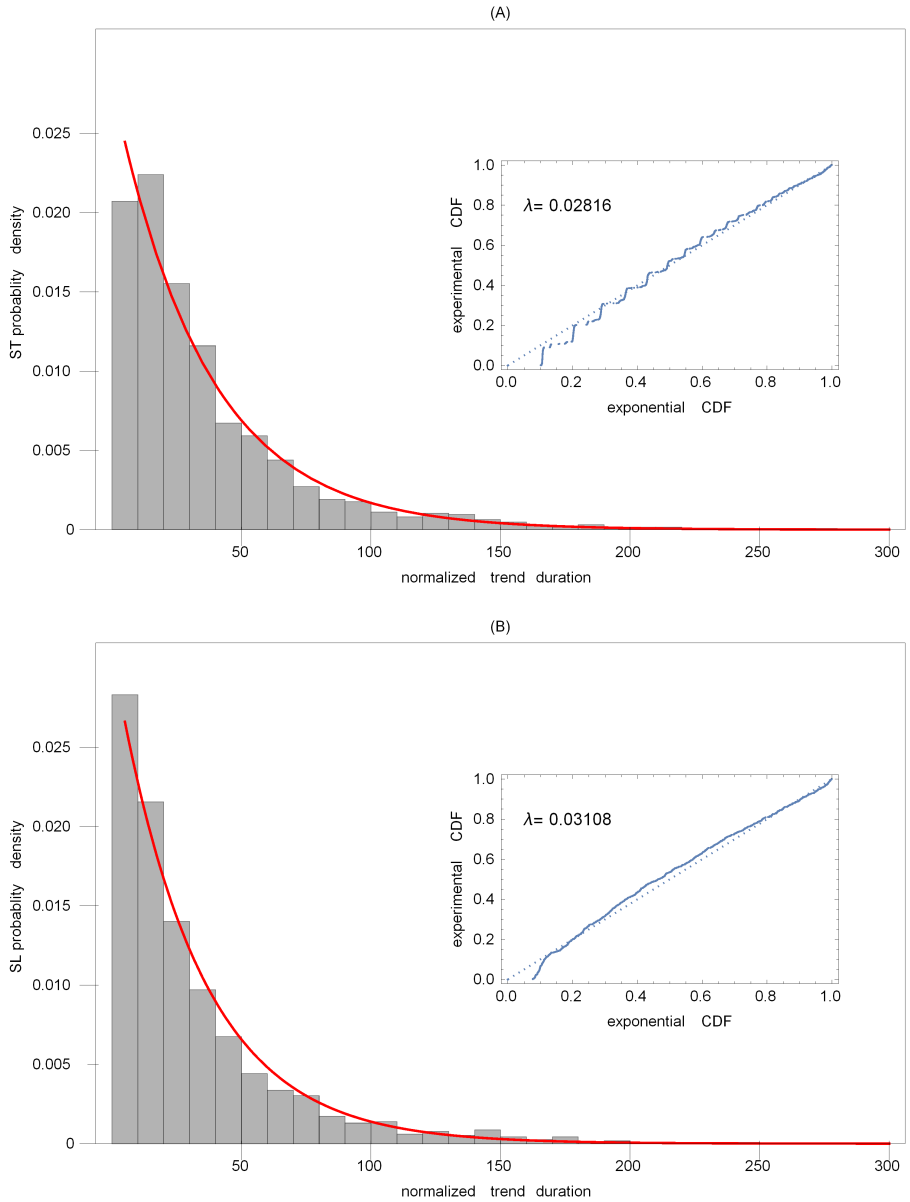

Fig 2. Probability density function (PDF) of normalized duration of trends for: (A) stride time (ST) and (B) stride length (SL). Trend durations turned out to be independent of treadmill's speed. Consequently, we created two aggregated data sets from trials at different speeds. The solid curves in both subplots show the best-fit exponential PDFs. The probability plots, presented as insets, show the differences between the experimental and exponential cumulative distribution functions (CDFs).

Table 1. Scaling exponents for spatio-temporal gait parameters. $\alpha^{(0)}$, $\alpha^{(1)}$, and $\alpha^{(2)}$ are exponents calculated using detrended fluctuation analysis of order 0 (DFA0), 1 (DFA1), and 2 (DFA 2), respectively. $\alpha^{(FA)}$ was computed using the fluctuation analysis algorithm (FA). Scaling analysis was performed for raw experimental time series and the time series detrended using the piecewise linear variant of the MARS model. In the latter case the exponents have a L subscript. All indices that are statistically smaller than 0.5 are marked with the dagger symbol.

PWS [%]	$\alpha^{(0)}$	$\alpha^{(1)}$	$\alpha^{(2)}$	$\alpha^{(FA)}$	$\alpha_L^{(0)}$	$\alpha_L^{(1)}$	$\alpha_L^{(2)}$	$\alpha_L^{(FA)}$
stride length								
80	0.76 ± 0.10	0.73 ± 0.12	0.69 ± 0.12	0.77 ± 0.10	$0.38 \pm 0.07\dagger$	0.52 ± 0.07	0.57 ± 0.08	$0.38 \pm 0.07\dagger$
90	0.71 ± 0.12	0.70 ± 0.11	0.67 ± 0.11	0.71 ± 0.11	$0.39 \pm 0.07\dagger$	0.53 ± 0.05	0.57 ± 0.06	$0.39 \pm 0.07\dagger$
100	0.75 ± 0.12	0.77 ± 0.14	0.70 ± 0.13	0.75 ± 0.12	$0.34 \pm 0.07\dagger$	0.49 ± 0.07	0.53 ± 0.08	$0.34 \pm 0.07\dagger$
110	0.73 ± 0.12	0.75 ± 0.15	0.70 ± 0.16	0.73 ± 0.11	$0.36 \pm 0.10\dagger$	0.50 ± 0.08	0.53 ± 0.08	$0.36 \pm 0.10\dagger$
120	0.75 ± 0.12	0.76 ± 0.14	0.71 ± 0.13	0.75 ± 0.11	$0.36 \pm 0.07\dagger$	0.52 ± 0.08	0.56 ± 0.09	$0.37 \pm 0.07\dagger$
stride time								
80	0.81 ± 0.10	0.81 ± 0.16	0.73 ± 0.16	0.82 ± 0.09	$0.38 \pm 0.07\dagger$	0.52 ± 0.07	0.56 ± 0.09	$0.38 \pm 0.07\dagger$
90	0.75 ± 0.10	0.79 ± 0.11	0.75 ± 0.13	0.77 ± 0.09	$0.37 \pm 0.07\dagger$	0.54 ± 0.07	0.59 ± 0.10	$0.37 \pm 0.07\dagger$
100	0.77 ± 0.11	0.85 ± 0.14	0.78 ± 0.15	0.77 ± 0.11	$0.36 \pm 0.10\dagger$	0.54 ± 0.10	0.59 ± 0.10	$0.36 \pm 0.10\dagger$
110	0.77 ± 0.10	0.82 ± 0.16	0.76 ± 0.20	0.77 ± 0.09	$0.36 \pm 0.07\dagger$	0.53 ± 0.09	0.57 ± 0.11	$0.36 \pm 0.07\dagger$
120	0.81 ± 0.10	0.83 ± 0.16	0.75 ± 0.17	0.81 ± 0.10	$0.36 \pm 0.08\dagger$	0.52 ± 0.09	0.57 ± 0.10	$0.36 \pm 0.08\dagger$
stride speed								
80	$0.44 \pm 0.08\dagger$	0.48 ± 0.07	0.50 ± 0.08	$0.45 \pm 0.07\dagger$	$0.42 \pm 0.07\dagger$	$0.46 \pm 0.07\dagger$	$0.47 \pm 0.07\dagger$	$0.42 \pm 0.07\dagger$
90	$0.41 \pm 0.08\dagger$	$0.47 \pm 0.07\dagger$	0.48 ± 0.07	$0.41 \pm 0.08\dagger$	$0.38 \pm 0.07\dagger$	$0.45 \pm 0.06\dagger$	$0.47 \pm 0.07\dagger$	$0.38 \pm 0.07\dagger$
100	$0.41 \pm 0.11\dagger$	$0.44 \pm 0.08\dagger$	$0.44 \pm 0.07\dagger$	$0.41 \pm 0.11\dagger$	$0.37 \pm 0.08\dagger$	$0.42 \pm 0.06\dagger$	$0.43 \pm 0.06\dagger$	$0.37 \pm 0.08\dagger$
110	$0.42 \pm 0.08\dagger$	$0.46 \pm 0.07\dagger$	$0.46 \pm 0.08\dagger$	$0.42 \pm 0.08\dagger$	$0.38 \pm 0.08\dagger$	$0.43 \pm 0.07\dagger$	$0.45 \pm 0.08\dagger$	$0.38 \pm 0.08\dagger$
120	0.49 ± 0.13	0.48 ± 0.07	0.49 ± 0.09	0.49 ± 0.12	$0.40 \pm 0.07\dagger$	$0.46 \pm 0.07\dagger$	$0.48 \pm 0.08\dagger$	$0.40 \pm 0.07\dagger$

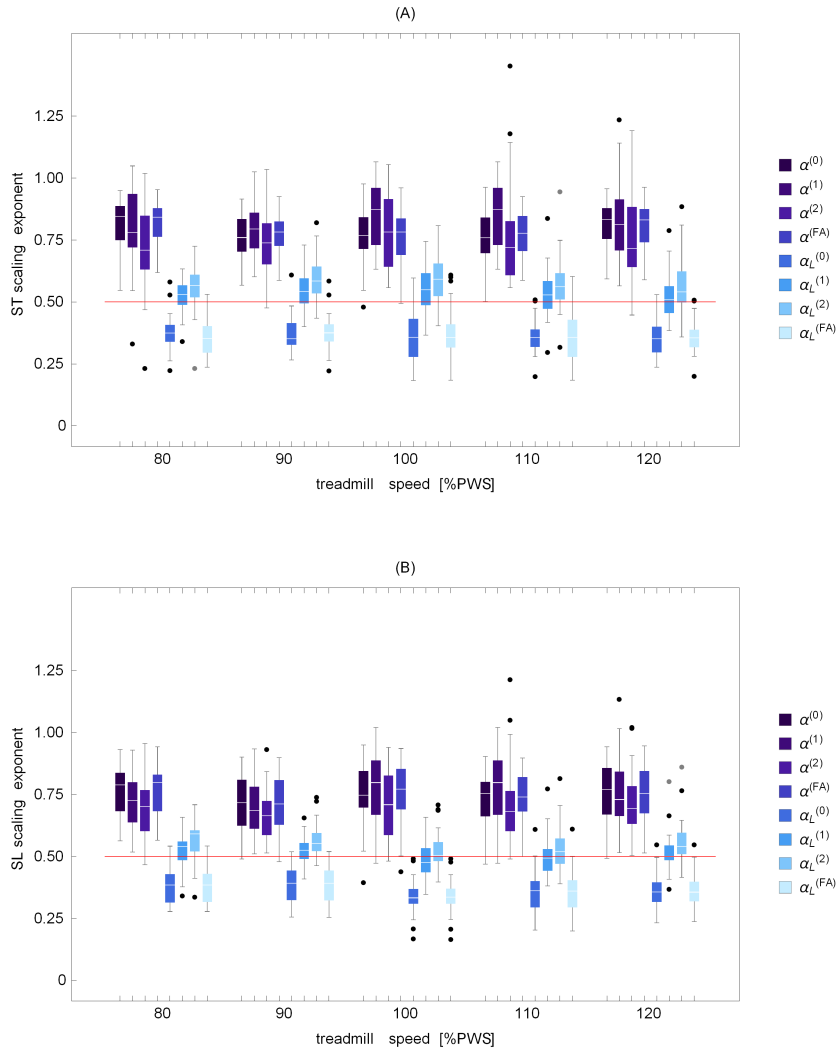

Fig 3. Scaling exponents of stride time (A) and stride length (B) as a function of treadmill speed. $\alpha^{(0)}$, $\alpha^{(1)}$, $\alpha^{(2)}$, and $\alpha^{(FA)}$ are exponents calculated using detrended fluctuation analysis of order 0 (DFA0), 1 (DFA1), 2 (DFA2), and FA, respectively. Calculations were performed for raw experimental time series and the time series detrended using the piecewise linear variant of the MARS model. In the latter case the exponents have a L subscript. The horizontal red line delineates persistent (> 0.5) and anti-persistent (< 0.5) scaling.

The scaling indices did not depend on treadmill's speed with only two exceptions. $\alpha_L^{(1)}$ and $\alpha_L^{(2)}$ for SL series at 80% PWS were different from those at 100% PWS ($p = 0.04$).

Apart from the lowest treadmill speed, the order of DFA detrending did not have a statistically significant effect on the values of the scaling exponents of original experimental time series. For stride length at 80% PWS, ANOVA gave $p = 0.02$. The

post hoc analysis showed that mean of $\alpha^{(0)} = 0.76$ was significantly greater than that of $\alpha^{(2)} = 0.69$. For stride time at 80% PWS, the Kruskal-Wallis test yields $p = 0.03$, but the post hoc analysis did not reveal any differences. In all but one case, the parameters $\alpha^{(0)}$, $\alpha^{(1)}$, and $\alpha^{(2)}$ were not different from $\alpha^{(FA)}$. For step length at 80% PWS, $\alpha^{(FA)} = 0.77$ was greater than $\alpha^{(2)} = 0.69$.

For all treadmill speeds and gait parameters, there were no differences between the scaling exponents $\alpha_L^{(0)}$ and $\alpha_L^{(FA)}$ of time series detrended using the MARS algorithm. There was also agreement between $\alpha_L^{(1)}$ and $\alpha_L^{(2)}$. In all the cases, the exponents determined using DFA1 and DFA2 were statistically different from those calculated with DFA0 and FA.

DFA0 and FA of MARS ST and SL residuals yielded indices $\alpha_L^{(0)}$ and $\alpha_L^{(FA)}$ that were significantly smaller than 0.5. Generally, the opposite was true for $\alpha_L^{(1)}$ and $\alpha_L^{(2)}$.

The stride speed scaling exponents determined with either DFAn or FA were smaller than 0.5 in the majority of cases.

To identify the origin of ST and SL persistence, we determined the piecewise linear MARS trends and the corresponding residuals for each trial. We then created an ensemble of 100 composite signals constructed from the original trends and randomly shuffled residuals. We performed DFA1 and DFA2 analysis on such ensembles. For both gait parameters and all treadmill speeds, $\alpha^{(1)}$ and $\alpha^{(2)}$ were greater than 0.5. Thus, the outcome of DFA was determined not by the properties of the surrogate noise, which was devoid of any correlations, but by the properties of trends. The results of such numerical experiment for the time series from Fig. 1 are displayed in Fig. 4.

For each detrended time series having the scaling exponent of $\alpha_L^{(FA)} < 0.5$ we used surrogate data to test whether fluctuations are indeed anti-persistent. In particular, we tested whether $\alpha_L^{(FA)}$ is smaller than either the median or mean of scaling exponents of 1000 time series generated by random shuffling. The outcome of this analysis is presented in Table 2. The overwhelming majority of time series were anti-persistent. For example, at preferred walking speed, 94% of the scaling exponents for stride speed were smaller than 0.5, and 87% of them were anti-persistent.

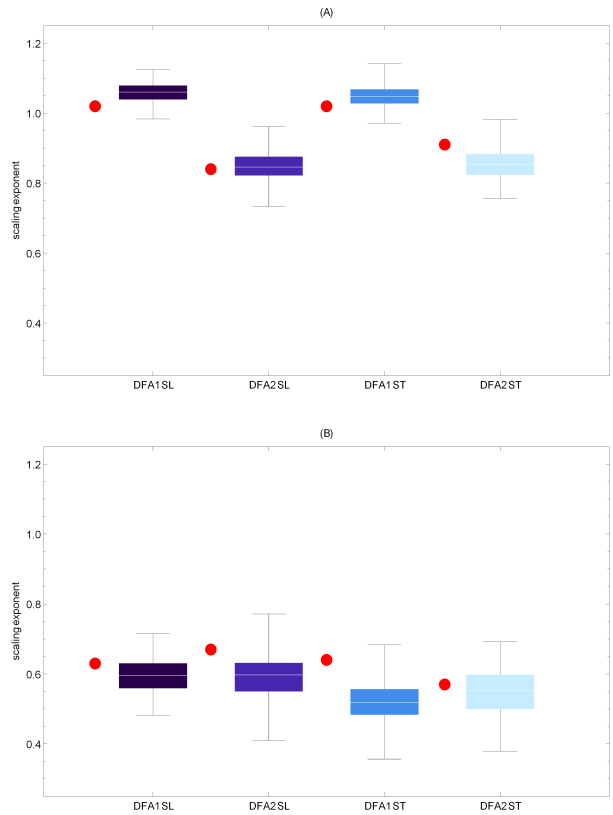

Fig 4. Boxplots of DFA1 ($\alpha^{(1)}$) and DFA2 ($\alpha^{(2)}$) scaling exponents for ensembles of signals comprised of MARS trends extracted from experimental time series and randomly shuffled corresponding MARS residuals. Red disks to the left of each boxplot represent the values of the scaling exponents of the original time series used to generate the ensembles. The calculations were carried out for both stride time (ST) and stride length (SL) time series shown in Fig. 1A and Fig. 1B. Even though there were no correlations in shuffled MARS residuals, the median values of $\alpha^{(1)}$ and $\alpha^{(2)}$ of the composite signals were significantly greater than 0.5 and similar to the scaling exponents of the original time series. Thus, this numerical experiment shows that DFA detrending is incapable of removing trends from ST and SL time series. The values of the scaling exponents of the experimental time series shown in Fig. 1A were: $\alpha^{(1)} = 1.02$ and $\alpha^{(2)} = 0.84$ for SL, and $\alpha^{(1)} = 1.02$ and $\alpha^{(2)} = 0.91$ for ST. For time series in Fig. 1B: $\alpha^{(1)} = 0.63$ and $\alpha^{(2)} = 0.67$ for SL, and $\alpha^{(1)} = 0.64$ and $\alpha^{(2)} = 0.57$ for ST.

Correlation coefficients

Fig. 5 shows the boxplots of Pearson's correlation coefficient ρ between stride time and stride length for all five speeds. Correlations were calculated for: experimental (raw) time series, trends determined using the MARS algorithm, and MARS residuals (noise).

Table 2. Percentage of trials for which the value of the scaling exponent $\alpha_L^{(FA)}$ for the MARS residuals of stride time (ST), stride length (SL), and stride speed (SS) were smaller than 0.5. In each case for which $\alpha_L^{(FA)} < 0.5$ we used surrogate data to verify that fluctuations were indeed anti-persistent.

PWS [%]	80	90	100	110	120
Scaling exponents smaller than 0.5 [%]					
SL	79	78	76	74	71
ST	91	78	82	82	79
SS	88	100	94	91	74
Anti-persistent scaling exponents [%]					
SL	81	84	84	68	83
ST	80	72	78	79	78
SS	76	78	87	84	88

ρ was independent of speed: $p_{raw} = 0.32$, $p_{trend} = 0.63$, and $p_{noise} = 0.24$. For the preferred walking speed (PWS) we obtain, $\rho_{raw} = 0.52 \pm 0.17$, $\rho_{trend} = 0.85 \pm 0.12$, and $\rho_{noise} = 0.20 \pm 0.16$. Thus, coupling between trends was determined to be very strong.

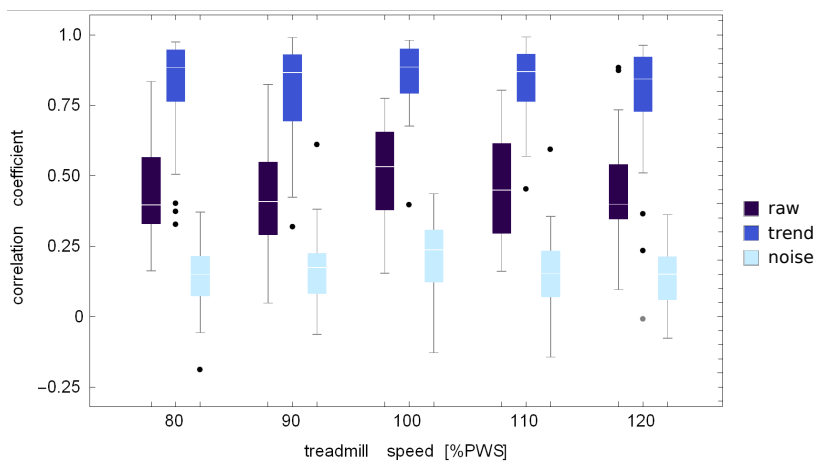

Fig 5. Pearson's correlation coefficient between stride time and stride length at five different speeds. Correlations were calculated for: experimental (raw) time series, trends determined using the MARS algorithm, and MARS residuals (noise).

Discussion

Detrended fluctuation analysis is one of the most frequently used algorithms for fractal analysis of experimental time series. At the time of writing, the seminal paper of Peng et al. [4] has been cited almost 1800 times. It is difficult to overestimate the importance of this method in general and in quantitative gait analysis in particular [1, 2, 14, 16–27].

Early on, numerical investigations showed that simple non-stationarities, such as

sinusoidal periodicity or monotonic global trends [28, 29], as well as more complex sources of non-stationarity [30], affected DFA estimates of the scaling exponent. Bryce and Sprague correctly pointed out that, paradoxically, rather than raising doubts about the purported universal applicability of DFA for trended processes, those papers were actually used to demonstrate the efficacy of the method [31].

In DFA, detrending is performed on the integrated signal. Consequently, global linear trends can be eliminated using second or higher order DFA [28, 32]. Figure 1A shows that prominent piecewise linear trends in stride time and stride length may appear even during treadmill walking. Thus, it is surprising that DFA1, which cannot mitigate even global linear trends, was used in most of the previous studies of scaling in spatio-temporal gait parameters. There are two possible explanations for the prevalence of DFA1 in gait analysis. First, while global linear trends distinctly manifest themselves as crossovers in DFA fluctuation function, no apparent crossovers are observed in gait data. Second, the scaling exponents determined using DFA1 and DFA2 are not statistically different, as is evident from the data collected in Table 1, as well as from the visualizations of their distributions in Fig. 3. This agreement was presumably used in favor of DFA1. We demonstrated that the order of DFA detrending did not have a statistically significant effect on the values of the scaling exponents of the experimental time series. Moreover, $\alpha^{(0)}$, $\alpha^{(1)}$, and $\alpha^{(2)}$ were not significantly different from $\alpha^{(FA)}$. Thus, we infer that DFA detrending is ineffective, and the observed persistence of ST and SL stems from the properties of trends. This interpretation is corroborated by the outcome of detrended fluctuation analysis of signals made up of original trends and randomly shuffled MARS residuals. The fact that the DFA scaling exponents of ST and SL were sharply greater than 0.5 provided additional evidence that the outcome of DFA was determined not by the properties of the surrogate noise, which was devoid of any correlations, but by the properties of the trends that DFA analysis was not able to eliminate.

Table 1 shows that the scaling exponents $\alpha_L^{(1)}$ and $\alpha_L^{(2)}$ of MARS residuals are somewhat larger than 0.5, in contrast to the values of $\alpha_L^{(0)}$ and $\alpha_L^{(FA)}$. These differences are not surprising, taking into account the spurious correlations that can be introduced by DFA detrending of nonlinear signals [31]. Herein, we used a piecewise linear approximation of ST and SL trends. While this approximation is good, as demonstrated

by Fig. 1A and the similar figures presented in the online supplement, the MARS residuals undoubtedly contain an admixture of the remnants of the original trends. Upon integration, such remnants make DFA fluctuation function nonlinear. As expected, there were no trends in tightly controlled stride speed. Consequently, there were no differences in the values of scaling exponents determined using DFA and FA.

We are not aware of any previous studies that explicitly analyze the properties of trends in human gait. The normalized trend durations of ST and SL have a quasi-exponential distribution – the probability distribution that describes the time between events in a Poisson point process, i.e. a process in which events occur continuously and independently at a constant average rate. The existence of trends is quite likely a manifestation of intermittent control. During typical motor control tasks such as walking, or quiet standing, the human central nervous system must handle multiple sources of dynamic instability. These include time delays, sensory uncertainty, endogenous motor noise, and gravitational toppling torques. Both the biological and the cybernetic rationale favors intermittent predictive control over continuous control processes, e.g., see [33, 34] and references therein. Future studies should determine whether the control of ST and SL is time- or event-driven. In other words, whether it results from discrete sampling or is triggered by an error crossing a threshold.

Humans have an innate ability to synchronize their movements with rhythmic sound stimuli. Sejdic et al. argue that sound associated with bipedal gait influenced the evolution of human auditory-motor rhythmic abilities [35]. Walking in sync with a metronome has previously been investigated as a potential rehabilitation tool in patients with Parkinson's disease [36] and stroke [37]. Isochronous metronome induces anti-persistence in stride time which raises doubts about the efficacy of such rehabilitation. Application of persistent metronomes to gait rehabilitation is an active field of research [20–23, 38]. Roerdink et al. asked a fundamental question [14]: how to sync to the beat of a persistent fractal metronome without falling off the treadmill? They argue that the increased coupling between ST and SL fluctuations inhibit large displacement along the treadmill. Herein, we found that even in the absence of fractal auditory cueing, the trends of ST and SL were strongly correlated (e.g. $\rho_{trend} = 0.85$ at PWS), and their corresponding residuals were anti-persistent. Thus, persistence of ST and SL time series does not not imply that these gait parameters are weakly controlled.

We hypothesize that the values of trends serve as instantaneous control points about which these gait parameters fluctuate with anti-persistent statistics.

It is worth pointing out that the ST-SL correlation coefficient for Dingwell's experimental data $\rho_{raw} \approx 0.50$ is about twice as large as that in the Roerdink et al. study [14]. The shorter treadmill (1.7 m) used by Dingwell et al. may account for increased ST-SL correlation.

Conclusions

Hausdorff et al. [1, 2] discovered long-range, persistent correlations in stride duration of human gait nearly a quarter century ago. This persistence was attributed to correlated noise superposed on dynamically irrelevant trends. The evidence presented herein necessitates a fundamental revision of such an interpretation: the persistence of gait parameters stems from the presence of trends and not from properties of motor control noise. We believe that better understanding of gait control mechanisms will pave the way for novel, more effective strategies of gait rehabilitation.

Herein, we proposed a novel approach to determination of scaling exponents of time series with trends – the combination of the MARS detrending and fluctuation analysis (MARS-FA). This algorithm is applicable to diverse time series generated by physical, social, or biological systems. We will present a MARS-FA scaling analysis of human heart rate variability and cerebral blood flow in a separate publication.

Materials and methods

Experimental data

In our analysis, we used data from the study of Dingwell et al. [15], which were available in the Dryad repository [39]. Seventeen young healthy adults were asked to walk on a motor-driven treadmill for five minutes, at five different speeds, determined as a percentage of a subject's preferred walking speed (PWS). There were two trials for each speed (80%, 90%, 100%, 110%, 120% PWS). SL, ST, and SS were determined using a motion capture system. A comprehensive description of the experimental protocol and participants' characteristics can be found in the original paper.

Multivariate Adaptive Regression Splines (MARS)

To model trends in spatio-temporal gait parameters we adopted MARS (Multivariate Adaptive Regression Splines) — nonparametric adaptive regression method proposed by J. Friedman [40, 41]. Let $\{y_i\}_{i=1}^N$ be a time series of experimental values observed at instances $\{x_i\}_{i=1}^N$. The MARS model f is a linear combination of basis functions h_m:

$$f(x) = \beta_0 + \sum_{m=1}^{M} \beta_m h_m(x). \tag{1}$$

We denote by $\mathcal{M}$ the set of basis functions h_m which are constructed in a very specific way. Let us consider two piecewise linear functions *max(0,x−t)* and *max(0,t-x)* with a knot at t. These two functions (linear splines) form a so called reflected pair. The example of such a pair is given in Fig 6. We begin the construction of $\mathcal{M}$ by creating a set C of N reflected pairs with knots equal to values x_i:

$$C = \{max(0, x - t), max(0, t - x)\}_{t \in \{x_1, x_2, \ldots, x_N\}}. \tag{2}$$

The MARS model is build iteratively. A new basis function h_{M+1} is the product of one of the already constructed basis functions h_l and one of the reflected pairs from set C:

$$\hat{\beta}_{M+1} h_l(x)\, max(0, x - x_j) + \hat{\beta}_{M+2} h_l(x)\, max(0, x_j - x), h_l \in \mathcal{M}. \tag{3}$$

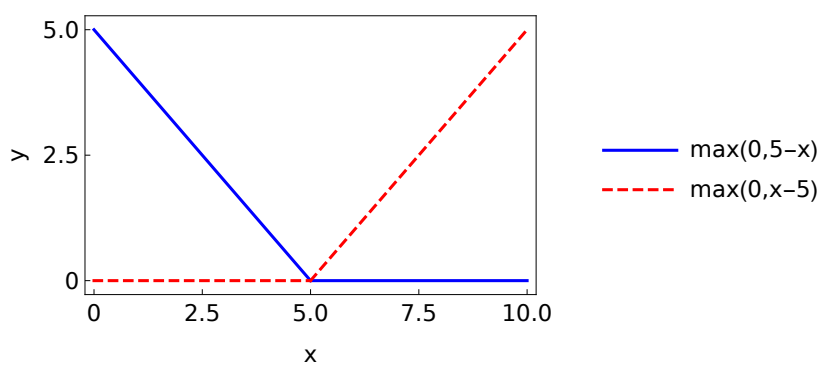

Fig 6. A pair of reflected basis functions with a knot at $t = 5$.

From all possible $(M + 1)N$ products of this form, we select the one that gives the maximum reduction in sum-of-squares residual error. Here $\hat{\beta}_{M+1}$ and $\hat{\beta}_{M+2}$ are coefficients estimated by least squares, along with all the other $M + 1$ coefficients in the

model. The first basis function $h_0(x)$ is constant equal to 1. The process of adding new terms, which is often called a forward model-building procedure (forward pass), is continued until the change in residual error is smaller than predefined stopping condition or until the maximum number of terms is reached.

The model built during the forward pass is usually overfitted and needs to be pruned to obtain better generalization ability. During each stage of a backward deletion procedure (backward pass), the term whose removal causes the smallest increase in residual squared error is deleted. In this way, we find the best model $\hat{f}_\lambda$ with λ terms. The goal of the pruning process is to minimize the value of generalized cross-validation:

$$GCV(\lambda) = \frac{\sum_{i=1}^{N}[y_i - \hat{f}_\lambda(x_i)]^2}{[1 - M(\lambda)/N]^2} \tag{4}$$

in order to estimate the optimal number of terms. $M(\lambda)$ is the effective number of parameters in the model:

$$M(\lambda) = r + cK \tag{5}$$

that accounts for both the number of linearly independent basis functions r and the number of knots K in the forward pass. c is a penalty for adding a new knot.

In this study, we used ARESLab, an open source MATLAB implementation of MARS [42], to approximate trends in gait spatiotemporal parameters using a piecewise linear, additive MARS model. In other words, every new basis function was just a linear combination of functions which belonged to a reflected pair (maximum order of interaction was equal to 1). The stopping condition for the forward phase was set to 0.001, and the generalized cross-validation knot penalty c was set equal to 2, the value most commonly used for additive models [41].

Scaling analysis

Detrended fluctuation analysis (DFA)

DFA was designed to detect long-time, power-law scaling of the second moment in the presence of additive, polynomial non-stationarity. Given a bounded time series $\{y_i\}_{i=1}^{N}$,

one creates an unbounded process

$$Y_t = \sum_{i=1}^{t} (y_i - < y >), \tag{6}$$

where $< y >$ denotes the mean value of the time series. Next, Y_t is divided into windows of length n and a local least-squares polynomial fit is performed within each window. Let P_t indicate the piece-wise sequence of such polynomial fits. Then, the root-mean-square deviation from the trend, the fluctuation function, is calculated:

$$F(n) = \sqrt{\frac{1}{N} \sum_{t=1}^{N} (Y_t - P_t)^2}. \tag{7}$$

A straight line on a log-log graph of $F(n)$ as a function of n is considered a manifestation of self-affinity as $F(n) \propto n^{\alpha}$. For fractional Gaussian noise, the exponent (index) α varies between 0 and 1. In this case, for $\alpha < 0.5$ fluctuations are anti-persistent and for $\alpha > 0.5$ they are persistent. The n-th order polynomial regression in the DFA family is typically denoted as DFAn. To facilitate reproducibility of the results, we used the Matlab function dfa from the WFDB Toolbox [43, 44] for DFA1 and DFA2 calculations.This function does not implement DFA0.

Fluctuation analysis (FA)

In fluctuation analysis [45], a precursor of DFA, the fluctuation function is computed as follows:

$$F(n) = \sqrt{\frac{1}{N-n} \sum_{t=1}^{N-n} (Y_{t+n} - Y_t)^2}, \tag{8}$$

and the scaling exponent is determined using the linear least squares fit on a log-log graph of $F(n)$.

Statistical analysis

We used the Shapiro-Wilk test to determine whether the analyzed data were normally distributed. The significance threshold for all the statistical tests was set to 0.05.

The dependence of trend durations of stride time and stride length on treadmill speed were examined with the Kruskal-Wallis test with Tukey's post hoc comparisons.

We compared the values of Pearson's correlation coefficient between stride time and stride length (experimental values, piecewise linear trends, and MARS residuals) at different speeds using ANOVA or the Kruskal-Wallis test (depending on normality of data). In both cases we used Tukey's post hoc comparisons.

For a given gait parameter and treadmill speed, the differences in scaling exponents determined using DFAn and FA were assessed with either ANOVA or the Kruskal-Wallis test (with Tukey's post hoc comparisons in both cases). Such statistical analysis was performed for both original and MARS detrended time series.

To determine whether fluctuations of spatio-temporal gait parameters were anti-persistent, we checked whether the corresponding scaling exponents were smaller than 0.5 using left-sided tests (t-test or the Wilcoxon signed rank test).

The Anderson-Darling test was used to compare ST and SL trend duration distributions and to verify whether these distributions were exponential.

The analysis of statistical properties of stride time and length trends was carried out using Mathematica 11.3 (Wolfram Research). The other calculations were performed with MATLAB R2016a (Mathworks).

Author Contributions

Conceptualization: Klaudia Kozlowska, Miroslaw Latka

Formal analysis: Klaudia Kozlowska, Miroslaw Latka, Bruce J. West

Investigation: Klaudia Kozlowska, Miroslaw Latka

Methodology: Klaudia Kozlowska, Miroslaw Latka, Bruce J. West

Software: Klaudia Kozlowska

Supervision: Miroslaw Latka

Validation: Miroslaw Latka

Visualization: Klaudia Kozlowska

Writing – original draft: Miroslaw Latka, Klaudia Kozlowska

Writing – review & editing: Bruce J. West

References

1. Hausdorff JM, Peng CK, Ladin Z, Wei JY, Goldberger AL. Is walking a random walk? Evidence for long-range correlations in stride interval of human gait. Journal of Applied Physiology. 1995;78(1):349–358. doi:10.1152/jappl.1995.78.1.349.

2. Hausdorff JM, Purdon PL, Peng CK, Ladin Z, Wei JY, Goldberger AL. Fractal dynamics of human gait: stability of long-range correlations in stride interval fluctuations. Journal of Applied Physiology. 1996;80(5):1448–1457. doi:10.1152/jappl.1996.80.5.1448.

3. Feder J. Fractals. Springer US; 1988. Available from: `https://doi.org/10.1007%2F978-1-4899-2124-6`.

4. Peng CK, Buldyrev SV, Havlin S, Simons M, Stanley HE, Goldberger AL. Mosaic organization of DNA nucleotides. Physical Review E. 1994;49(2):1685–1689. doi:10.1103/physreve.49.1685.

5. Goldberger AL, Rigney DR, West BJ. Science in Pictures: Chaos and Fractals in Human Physiology. Scientific American. 1990;262(2):42–49. doi:10.1038/scientificamerican0290-42.

6. Bassingthwaighte JB, Liebovitch LS, West BJ. Fractal Physiology. Springer New York; 1994. Available from: `https://doi.org/10.1007%2F978-1-4614-7572-9`.

7. West BJ. Fractal physiology and the fractional calculus: a perspective. Frontiers in Physiology. 2010;1. doi:10.3389/fphys.2010.00012.

8. Peng CK, Buldyrev SV, Hausdorff JM, Havlin S, Mietus JE, Simons M, et al. Non-equilibrium dynamics as an indispensable characteristic of a healthy biological system. Integrative Physiological and Behavioral Science. 1994;29(3):283–293. doi:10.1007/bf02691332.

9. Hausdorff J, Mitchell S, Firtion R, Peng C, Cudkowicz M, Wei J, et al. Altered fractal dynamics of gait: reduced stride-interval correlations with aging and Huntington's disease. J Appl Physiol (1985). 1997;82:262–9.

10. Goldberger A, Amaral L, Hausdorff J, Ivanov P, Peng C, Stanley H. Fractal dynamics in physiology: alterations with disease and aging. Proc Natl Acad Sci U S A. 2002;99 Suppl 1:2466–72.

11. Delignières D, Torre K. Fractal dynamics of human gait: a reassessment of the 1996 data of Hausdorff et al. Journal of Applied Physiology. 2009;106(4):1272–1279. doi:10.1152/japplphysiol.90757.2008.

12. Terrier P, Dériaz O. Persistent and anti-persistent pattern in stride-to-stride variability of treadmill walking: Influence of rhythmic auditory cueing. Human Movement Science. 2012;31(6):1585–1597. doi:10.1016/j.humov.2012.05.004.

13. Terrier P. Fractal Fluctuations in Human Walking: Comparison Between Auditory and Visually Guided Stepping. Annals of Biomedical Engineering. 2016;44(9):2785–2793. doi:10.1007/s10439-016-1573-y.

14. Roerdink M, Daffertshofer A, Marmelat V, Beek PJ. How to Sync to the Beat of a Persistent Fractal Metronome without Falling Off the Treadmill? PLOS ONE. 2015;10(7):e0134148. doi:10.1371/journal.pone.0134148.

15. Dingwell JB, Cusumano JP. Re-interpreting detrended fluctuation analyses of stride-to-stride variability in human walking. Gait & Posture. 2010;32(3):348–353. doi:10.1016/j.gaitpost.2010.06.004.

16. Terrier P, Turner V, Schutz Y. GPS analysis of human locomotion: Further evidence for long-range correlations in stride-to-stride fluctuations of gait parameters. Human Movement Science. 2005;24(1):97–115. doi:10.1016/j.humov.2005.03.002.

17. Jordan K, Challis JH, Newell KM. Walking speed influences on gait cycle variability. Gait & Posture. 2007;26(1):128–134. doi:10.1016/j.gaitpost.2006.08.010.

18. Hausdorff JM. Gait dynamics fractals and falls: Finding meaning in the stride-to-stride fluctuations of human walking. Human Movement Science. 2007;26(4):555–589. doi:10.1016/j.humov.2007.05.003.

19. Lamoth CJ, van Deudekom FJ, van Campen JP, Appels BA, de Vries OJ, Pijnappels M. Gait stability and variability measures show effects of impaired cognition and dual tasking in frail people. Journal of NeuroEngineering and Rehabilitation. 2011;8(1). doi:10.1186/1743-0003-8-2.

20. Kaipust JP, McGrath D, Mukherjee M, Stergiou N. Gait Variability is Altered in Older Adults When Listening to Auditory Stimuli with Differing Temporal Structures. Annals of Biomedical Engineering. 2013;41(8):1595–1603. doi:10.1007/s10439-012-0654-9.

21. Rhea C, Kiefer A, Wittstein M, Leonard K, MacPherson R, Wright W, et al. Fractal gait patterns are retained after entrainment to a fractal stimulus. PLoS One. 2014;9:e106755.

22. Rhea CK, Kiefer AW, D'Andrea SE, Warren WH, Aaron RK. Entrainment to a real time fractal visual stimulus modulates fractal gait dynamics. Human Movement Science. 2014;36:20–34. doi:10.1016/j.humov.2014.04.006.

23. Marmelat V, Torre K, Beek PJ, Daffertshofer A. Persistent Fluctuations in Stride Intervals under Fractal Auditory Stimulation. PLoS ONE. 2014;9(3):e91949. doi:10.1371/journal.pone.0091949.

24. Moon Y, Sung J, An R, Hernandez ME, Sosnoff JJ. Gait variability in people with neurological disorders: A systematic review and meta-analysis. Human Movement Science. 2016;47:197–208. doi:10.1016/j.humov.2016.03.010.

25. Kuznetsov N, Rhea C. Power considerations for the application of detrended fluctuation analysis in gait variability studies. PLoS One. 2017;12:e0174144.

26. Choi J, Kang D, Seo J, Tack G. Fractal fluctuations in spatiotemporal variables when walking on a self-paced treadmill. J Biomech. 2017;65:154–160.

27. Ducharme S, Liddy J, Haddad J, Busa M, Claxton L, van ER. Association between stride time fractality and gait adaptability during unperturbed and asymmetric walking. Hum Mov Sci. 2018;58:248–259.

28. Kantelhardt JW, Koscielny-Bunde E, Rego HHA, Havlin S, Bunde A. Detecting long-range correlations with detrended fluctuation analysis. Physica A: Statistical

Mechanics and its Applications. 2001;295(3-4):441–454. doi:10.1016/s0378-4371(01)00144-3.

29. Hu K, Ivanov PC, Chen Z, Carpena P, Stanley HE. Effect of trends on detrended fluctuation analysis. Physical Review E. 2001;64(1). doi:10.1103/physreve.64.011114.

30. Chen Z, Ivanov PC, Hu K, Stanley HE. Effect of nonstationarities on detrended fluctuation analysis. Physical Review E. 2002;65(4). doi:10.1103/physreve.65.041107.

31. Bryce RM, Sprague KB. Revisiting detrended fluctuation analysis. Scientific Reports. 2012;2(1). doi:10.1038/srep00315.

32. Bashan A, Bartsch R, Kantelhardt JW, Havlin S. Comparison of detrending methods for fluctuation analysis. Physica A: Statistical Mechanics and its Applications. 2008;387(21):5080–5090. doi:10.1016/j.physa.2008.04.023.

33. Gawthrop P, Loram I, Lakie M, Gollee H. Intermittent control: a computational theory of human control. Biological Cybernetics. 2011;104(1-2):31–51. doi:10.1007/s00422-010-0416-4.

34. Yoshikawa N, Suzuki Y, Kiyono K, Nomura T. Intermittent Feedback-Control Strategy for Stabilizing Inverted Pendulum on Manually Controlled Cart as Analogy to Human Stick Balancing. Frontiers in Computational Neuroscience. 2016;10(April). doi:10.3389/fncom.2016.00034.

35. Sejdić E, Fu Y, Pak A, Fairley JA, Chau T. The effects of rhythmic sensory cues on the temporal dynamics of human gait. PLoS ONE. 2012;7(8). doi:10.1371/journal.pone.0043104.

36. Suteerawattananon M, Morris G, Etnyre B, Jankovic J, Protas E. Effects of visual and auditory cues on gait in individuals with Parkinson's disease. Journal of the neurological sciences. 2004;219(1-2):63–69.

37. Roerdink M, Lamoth CJ, van Kordelaar J, Elich P, Konijnenbelt M, Kwakkel G, et al. Rhythm perturbations in acoustically paced treadmill walking after stroke. Neurorehabilitation and Neural Repair. 2009;23(7):668–678.

38. Hunt N, McGrath D, Stergiou N. The influence of auditory-motor coupling on fractal dynamics in human gait. Scientific Reports. 2014;4(1). doi:10.1038/srep05879.

39. Dingwell JB, Cusumano JP. Data from: Do humans optimally exploit redundancy to control step variability in walking? Dryad Digital Repository.; 2015. Available from: `http://dx.doi.org/10.5061/dryad.sk55m`.

40. Friedman JH. Multivariate Adaptive Regression Splines. The Annals of Statistics. 1991;19(1):1–67. doi:10.1214/aos/1176347963.

41. Hastie T, Tibshirani R, Friedman J. The Elements of Statistical Learning. Springer New York; 2009. Available from: `https://doi.org/10.1007%2F978-0-387-84858-7`.

42. Jēkabsons G. ARESLab: Adaptive Regression Splines toolbox; 2016. Available from: `http://www.cs.rtu.lv/jekabsons/regression.html`.

43. Moody GB, Mark RG, Goldberger AL. PhysioNet: a research resource for studies of complex physiologic and biomedical signals. In: Computers in Cardiology 2000. Vol.27 (Cat. 00CH37163). IEEE;.Available from: `https://doi.org/10.1109%2Fcic.2000.898485`.

44. Silva I, Moody GB. An Open-source Toolbox for Analysing and Processing PhysioNet Databases in MATLAB and Octave. Journal of Open Research Software. 2014;2. doi:10.5334/jors.bi.

45. Peng CK, Buldyrev SV, Goldberger AL, Havlin S, Sciortino F, Simons M, et al. Long-range correlations in nucleotide sequences. Nature. 1992;356(6365):168–170. doi:10.1038/356168a0.